

# Miscibility, Water Uptake, Ion Exchange Capacity, Conductivity and Dielectric Studies of Poly(methyl methacrylate) and Cellulose Acetate Blends

H. S. Sreekantha Jois, Denthaje Krishna Bhat

Department of Chemistry, National Institute of Technology Karnataka, Surathkal, Srinivasnagar 575025, India  
Correspondence to: D. K. Bhat (E-mail: denthajekb@gmail.com).

**ABSTRACT:** In the last few decades, polymer blends with good miscibility and conductivity have been the focus of study for material scientists. Here, polymer blends of Poly(methyl methacrylate) (PMMA) and Cellulose acetate (CA) of varying blend compositions have been prepared by solution casting method and their miscibility, water uptake, ion exchange capacity (IEC) proton conductivity, and dielectric properties have been studied. Dimethyl formamide (DMF) was used as solvent. Fourier transform infrared spectra (FTIR) and Differential scanning calorimetry (DSC) measurements have been used to analyze the miscibility of the blends. Up to 50/50 PMMA/CA, water uptake showed an increasing trend and for other compositions the value decreased. Ion exchange capacity and conductivity of the blends decreased with increase in PMMA content of the blends. The variations in the blend properties have been attributed to the presence of specific interactions and exchangeable groups in the blend system. The proton conductivity of the blends is in the order of  $10^{-3}$  S cm<sup>-1</sup>. Impedance analysis of the blends indicated the absence of any relaxation phenomenon in the blend system. © 2013 Wiley Periodicals, Inc. *J. Appl. Polym. Sci.* 130: 3074–3081, 2013

**KEYWORDS:** blends; differential scanning calorimetry (DSC); properties and characterization

Received 25 June 2012; accepted 10 May 2013; Published online 8 June 2013

**DOI:** 10.1002/app.39535

## INTRODUCTION

The quest for new polymer materials with desirable properties is ever increasing. This is mainly due to the flexibility and tailorable properties exhibited by these amazing materials. Polymer blending is a very useful and also an attractive tool to obtain new polymeric materials with more balanced properties than their components. Thermodynamically, the presence of hydrogen-bonding interactions between proton donor and acceptor polymers can improve the miscibility of their blends.<sup>1,2</sup> In general, the blend polymers possess intermediate chemical, physical, mechanic, and morphological properties of the component polymers. Hence, advantages from each polymer can be combined by blending two or more polymers.

Different structural systems can be produced when polymers are mixed, depending on the affinity of the components involved.<sup>3</sup> The final properties of polymer blends are directly related to the quality of their morphology, which in turn depends on the rheological properties of the phases of the blend, on the composition of the blend, on the processing conditions of the blend, and on the miscibility between the polymers forming the blend.<sup>4</sup> Polymer blends containing at least one biodegradable polymer component are referred to as bioblends. Products under active development from bioblends include those for (a) materials for packaging applications; (b) drug delivery systems and (c) cell culture/tissue engineering applications.<sup>5</sup>

Poly (methyl methacrylate) (PMMA) is a nonbiodegradable polymer with good transparency and mechanical strength. PMMA is the most commonly used polymer among the methacrylate family and has found tremendous applications in automotive and home appliances. Cellulose acetate (CA) is one of the most important derived natural polymer and hence can be susceptible to biodegradation. Therefore, the polymer blends of PMMA and CA can make suitable materials for many key applications where biodegradation is desirable. Hence it is of interest to study the properties of these blends. In view of these aspects and as a part of our ongoing research work on polymer blends and composites,<sup>6–9</sup> polyblends of PMMA and CA have been prepared by solution casting method. FTIR-ATR and DSC have been used to analyze the miscibility and existence of specific interactions in the blends. The water uptake, ion-exchange capacity and proton conductivity behavior of the blends have also been studied.

## EXPERIMENTAL

### Materials

Polymers tested in this work were obtained from commercial sources and were used as received. PMMA, with  $M_w = 1,20,000$  (Polydispersity = 1.05) and CA, with  $M_w = 52,000$  (Polydispersity < 1.10) were supplied by Sigma Aldrich. Dimethyl formamide (DMF) was used as solvent.

### Preparation of Blends

Blends of PMMA with CA were prepared by solution casting. The % (w/v) stock solutions of PMMA and CA were prepared in DMF by stirring for 24 h. The solution mixtures thus prepared were stirred for three hours for uniform mixing. They were then poured into Teflon petri dishes and the solvent was allowed to evaporate at 60°C for 72 h in a vacuum oven. The dried films were taken out and stored in a vacuum desiccator.

### MEMBRANE CHARACTERIZATION

#### Nuclear Magnetic Resonance Spectroscopic (NMR) and Fourier Transform Infrared (FTIR) Spectroscopic Studies

NMR spectra of PMMA samples were taken in a Bruker DPX-300 instrument at room temperature using CDCl<sub>3</sub> as solvent. FTIR spectra of the PMMA, CA and PMMA/CA blends were scanned in the range between 4000 and 400 cm<sup>-1</sup> on a NICO-LET AVATAR 330 FTIR-ATR spectrophotometer.

#### Differential Scanning Calorimetry (DSC) Studies

DSC thermograms of PMMA, CA, and PMMA/CA blends were obtained on a SHIMADZU DSC-60. The sample of 4–4.5 mg in weight was sealed in an aluminum pan and measurements were performed over the temperature range of ambient to 250°C at the heating rate of 10°C min<sup>-1</sup> under nitrogen gas flow.

#### Water Uptake

The water uptake in the PMMA/CA blends was measured by immersing the blends into deionized water at room temperature for 24 h. Then the blends were taken out, gently pressed with tissue paper, and immediately weighed on a balance. Triplicates were run for each blend to get the satisfactory reproducibility.<sup>6</sup> The water uptake in the blends,  $W$ , was calculated by

$$W = \frac{W_{\text{wet}} - W_{\text{dry}}}{W_{\text{dry}}} \quad (1)$$

where  $W_{\text{dry}}$  and  $W_{\text{wet}}$  are the weight of dry and corresponding water absorbed membranes, respectively.

#### Ion Exchange Capacity Measurements

Ion exchange capacity (IEC) indicates the number of milliequivalents (mequiv.) of ions in 1 g of the dry polymer blend. To determine the ion exchange capacity, blends of similar weight were soaked in 50 mL of 0.01N sodium hydroxide (NaOH) solution for 24 h at ambient temperature. After 24 h, 10 mL of the solution was titrated with 0.01N sulphuric acid (H<sub>2</sub>SO<sub>4</sub>), using a phenolphthalein indicator. IEC was calculated by

$$\text{IEC} = \frac{(B-P) \times 0.01 \times 5}{m} \quad (2)$$

where IEC is ion exchange capacity (in mequiv g<sup>-1</sup>),  $B$  is amount of sulphuric acid used to neutralize blank sample solution in mL.  $P$  is amount of H<sub>2</sub>SO<sub>4</sub> used to neutralize the blend soaked solution used in the study in mL, 0.01 is normality of the H<sub>2</sub>SO<sub>4</sub>. Here, 5 is the factor corresponding to the ratio of the amount of NaOH used to soak the blend/s to the amount used for titration, and  $m$  is the mass of the polymer blend in g.<sup>10</sup>

#### Electrochemical Impedance Spectroscopy and Proton Conductivity Measurement

The AC impedance spectra of the membranes were recorded in the frequency range between 0.01 Hz and 100,000 Hz with

amplitude of 5 mV using AUTOLAB Electrochemical System (Eco Chemie BV, Netherlands) over the temperature range of 30 °C to 70 °C. Proton conductivity measurements were performed on the membranes in a typical two-electrode cell by AC impedance technique. The conductivity cell composed of two copper electrodes of 2 cm × 2 cm dimensions. The blend sample was sandwiched between the two copper electrodes fixed in a Teflon block and kept in a closed glass container. 1M NaCl solution was used as an electrolyte. The cell was kept at each measuring temperature for a minimum of 60 min to ensure thermal equilibration of the sample at the temperature before measurement. The resistance value associated with the blend conductivity was determined from the high frequency intercept of the impedance with the real axis. The blend conductivity was calculated from the membrane resistance,  $R$ , using the following equation:

$$\sigma = L/RA \quad (3)$$

where  $\sigma$  is the proton conductivity of blend (in S cm<sup>-1</sup>),  $L$  is the thickness (in cm), and  $A$  is the area of the blend (in cm<sup>2</sup>).

#### Dielectric Studies

Complex impedance data,  $Z^*$  can be represented by its real,  $Z_R$  and imaginary,  $Z_I$  parts by the relation:

$$Z^* = Z_R + jZ_I \quad (4)$$

The relationships between complex impedance, admittance, permittivity, and electrical modulus can be found elsewhere.<sup>9</sup>

The equations for the dielectric constant,  $\epsilon_R$  and the dielectric loss,  $\epsilon_I$ , can be shown as

$$\epsilon_R = \frac{Z_I}{\omega C_0 (Z_R^2 + Z_I^2)} \quad (5)$$

$$\epsilon_I = \frac{Z_R}{\omega C_0 (Z_R^2 + Z_I^2)} \quad (6)$$

Here  $C_0 = \frac{\epsilon_0 A}{t}$  and  $\epsilon_0$  is the permittivity of the free space,  $A$  is the electrolyte-electrode contact area and  $t$  is the thickness of the sample and  $\omega = 2\pi f$ ,  $f$  being the frequency in Hz.

## RESULTS AND DISCUSSION

### NMR and FTIR Spectroscopic Studies

NMR scans of the PMMA samples were taken in order to verify the complete removal of the solvent from the prepared films. The NMR plot before drying showed a weak signal at a chemical shift value of 8.02 ppm showing the presence of DMF. This was absent in the NMR plot taken after the completion of drying process. Hence it can be concluded that the solvent DMF is not present in the blend films studied in this paper. NMR spectrum can also be used for determining the microstructure of the polymer. NMR traces of the PMMA film is shown in Figure 1. The presence of a methyl singlet at a chemical shift value of 0.84ppm indicated that the major part of polymer microstructure is syndiotactic. This observation is also supported by the experimentally obtained  $T_g$  value of 107.46°C for the polymer and literature reports.<sup>11–13</sup>

FTIR spectroscopy is used to check the presence of hydrogen bonding and the miscibility of the blends in the solid state. In comparison with the typical chemical changes, the changes in energies, bond lengths, and electron densities associated with

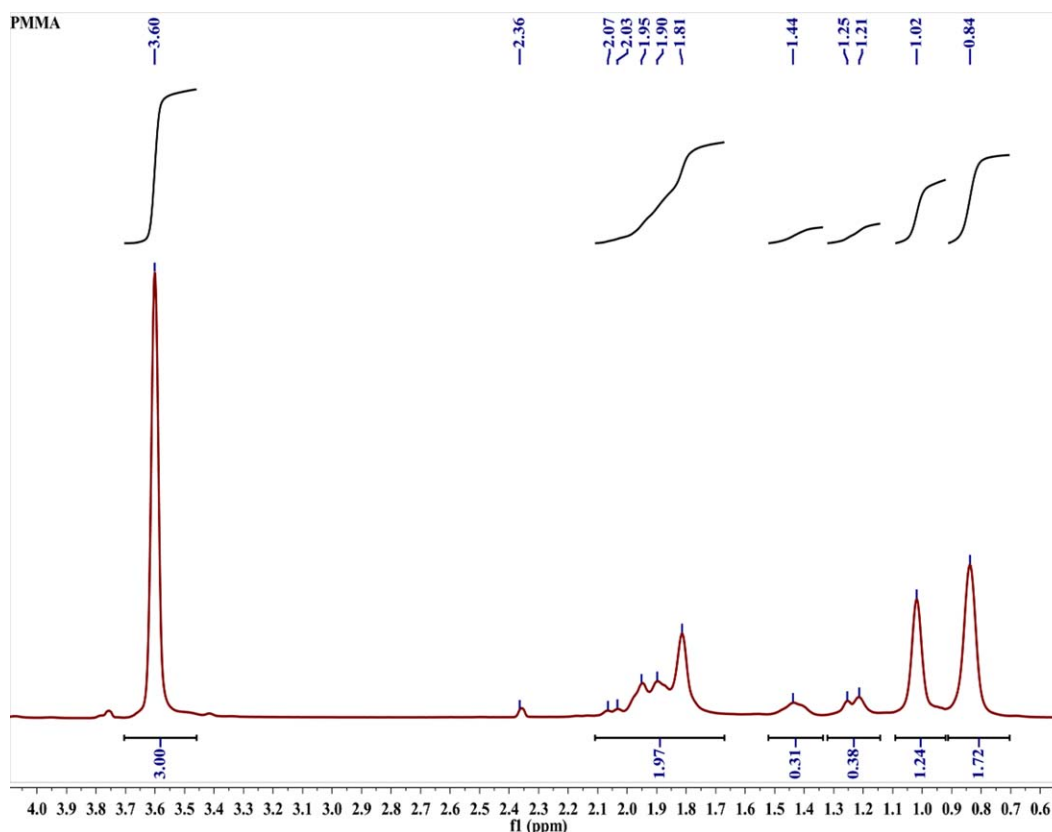


**Figure 1.** NMR trace of PMMA. [Color figure can be viewed in the online issue, which is available at [wileyonlinelibrary.com](http://wileyonlinelibrary.com).]

the formation of hydrogen bonds are actually quite small in magnitude. In spite of this, FTIR spectroscopy is very sensitive to the formation of the hydrogen bond.<sup>14</sup>

In general, when hydrogen bond formation occurs between two groups, the vibration frequencies of both the groups are expected to show a red shift compared with the free noninteracting group frequencies. This is also expected in a polymer blend made of polymers consisting of carbonyl and hydroxyl moieties as in the present case where PMMA has carbonyl group and the CA has both the carbonyl and hydroxyl groups. FTIR spectra of pure PMMA, PMMA/CA 50/50 blend and pure CA are shown in Figure 2(a–c), respectively.

The carbonyl frequency of pure CA [Figure 2(c)] at  $1736.4\text{ cm}^{-1}$  decreased to  $1723.1\text{ cm}^{-1}$  in the PMMA/CA 50/50 blend [Figure 2(b)], indicating the formation of a weak hydrogen bond between component polymers in the blend. This can be contributing to the miscibility of the blends. The strong and broad band at around  $3475.2\text{ cm}^{-1}$  and  $3610.3\text{ cm}^{-1}$  in pure CA and PMMA/CA 50/50 blend respectively, corresponded to the —OH stretching vibrations of hydroxyl groups. The intensity of the broad band decreased after blending, indicating that part of the —OH groups were involved in the hydrogen bond formation. These results indicate that the forces that exist in the blends may be due to the weak hydrogen bonding interactions. The C=O and —OH stretching frequencies of the pure and PMMA/CA blends are tabulated in Table I.

### DSC Studies

Miscibility of blends has been widely discussed in the literature. DSC is one of the standard methods employed to understand the miscibility of polymer blends. The DSC thermograms of pure PMMA and CA and PMMA/CA blends are shown in Figures 3 and 4, respectively.

From Figure 3, it can be seen that the  $T_g$  for pure CA and PMMA is  $190.38^\circ\text{C}$  and  $107.46^\circ\text{C}$ , respectively. It is interesting to note here that the thermograms for the blends (Figure 4) exhibited single  $T_g$  and its value lies intermediate to the  $T_g$  values of pure PMMA and pure CA. Further, the  $T_g$  values of the blend films decreased regularly on increase of PMMA content in the blends. Such a systematic variation of  $T_g$  in the blends is indicative of miscibility of the components in the blends.

A number of theoretical equations have been proposed for estimating the glass transition temperature of blend films from the properties of the pure components. Gordon-Taylor equation<sup>15,16</sup> [eq. (7)] and Fox equation<sup>6,17</sup> [eq. (8)] are the frequently used expressions for predicting the glass transition temperature of amorphous polymer blends:

$$T_g^b = \frac{W_1 T_{g1} + k W_2 T_{g2}}{W_1 + k W_2} \quad (7)$$

$$\frac{1}{T_g^b} = \frac{W_1}{T_{g1}} + \frac{W_2}{T_{g2}} \quad (8)$$

where  $T_g^b$  is glass transition temperature ( $T_g$ ) of the blend,  $T_{g1}$  and  $T_{g2}$  are the glass transition temperatures of the pure

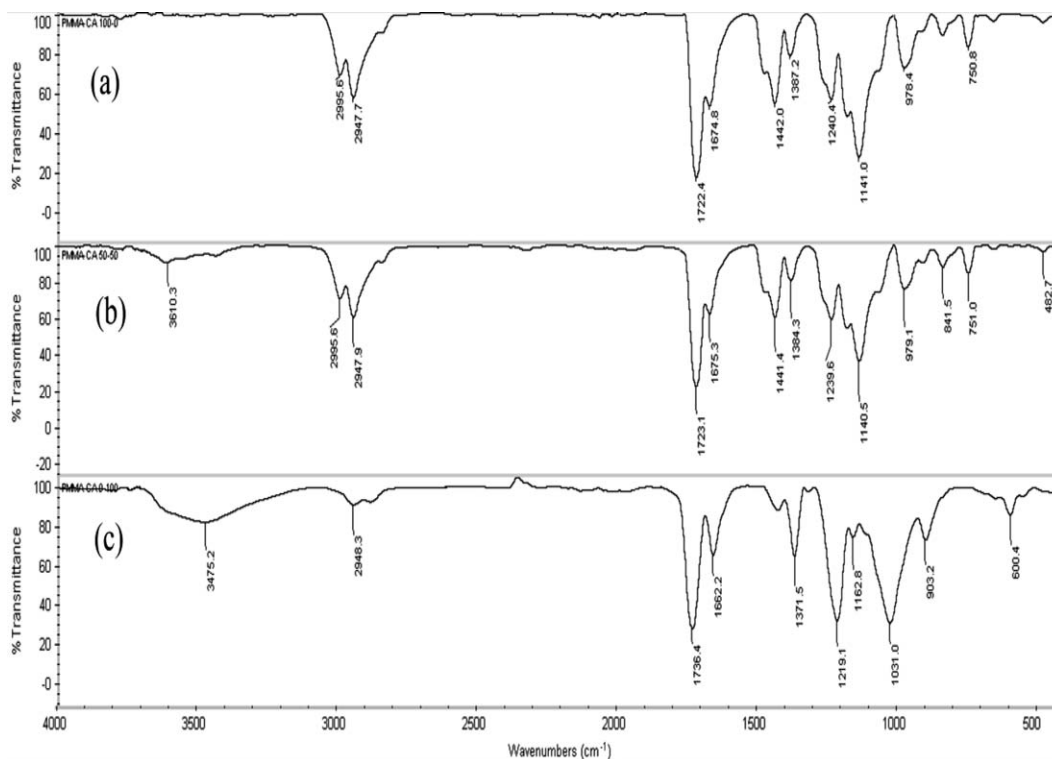


Figure 2. FTIR spectra of (a) Pure PMMA, (b) PMMA (50%)—CA (50%) blend and (c) Pure CA.

components, PMMA and CA respectively.  $W_1$  and  $W_2$  are weight fraction of components, PMMA and CA respectively.  $k$  is a fitting parameter and the experimental data is best fitted by this equation with  $k = 0.24$ . This result supports that PMMA/CA blends have high miscibility in the amorphous state. The thermal properties of PMMA/CA blends are represented in Table II.

The blends show a positive deviation from Fox equation implying an intermolecular interaction between the polymers.

#### Water Uptake

The relationship between water uptake and PMMA content in the blends is shown in Figure 5.

The water uptake of the blends increased upto 50 wt % of PMMA concentration. The maximum water uptake of 6.73% was observed for the blend with 50 wt % PMMA. The water absorption decreased on addition of further amounts of PMMA. In general, an increase in water uptake indicates the presence of voids in the polymer structure. The increase in water uptake in the blends up to 50wt.% of PMMA indicates that the blends are being formed with gradual increase in the void volume in the blends. The film appears slightly cloudy after water absorption. And this is maximum in the case of 50% CA blend film. At this composition the structure of the blend formed may be with maximum amount of void spaces. The hydrogen bonding between the components of the blends

Table I. IR Stretching Frequencies of Pure and PMMA/CA Blends

PMMA/CA (%)	C=O stretching frequency	—OH stretching frequency
0/100	1736.4	3475.2
10/90	1729.6	3460.2
20/80	1726.6	3471.4
30/70	1724.5	3443.8
40/60	1726.6	3479.1
50/50	1723.1	3610.3
60/40	1723.2	3617.0
70/30	1723.5	3619.2
80/20	1723.4	3615.8
90/10	1723.5	3608.0
100/0	1722.7	-

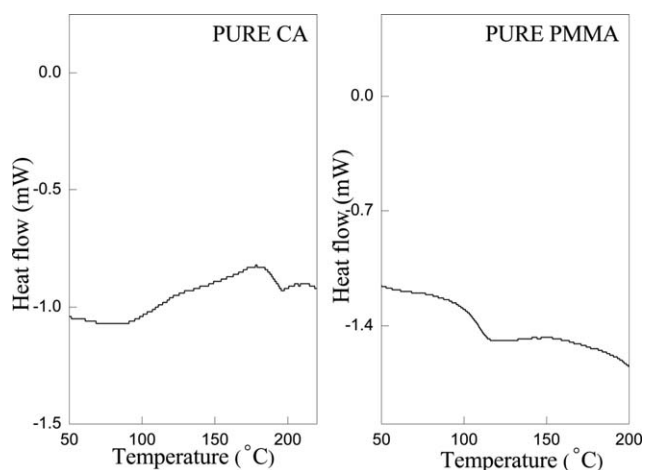


Figure 3. DSC scans of pure PMMA and pure CA.

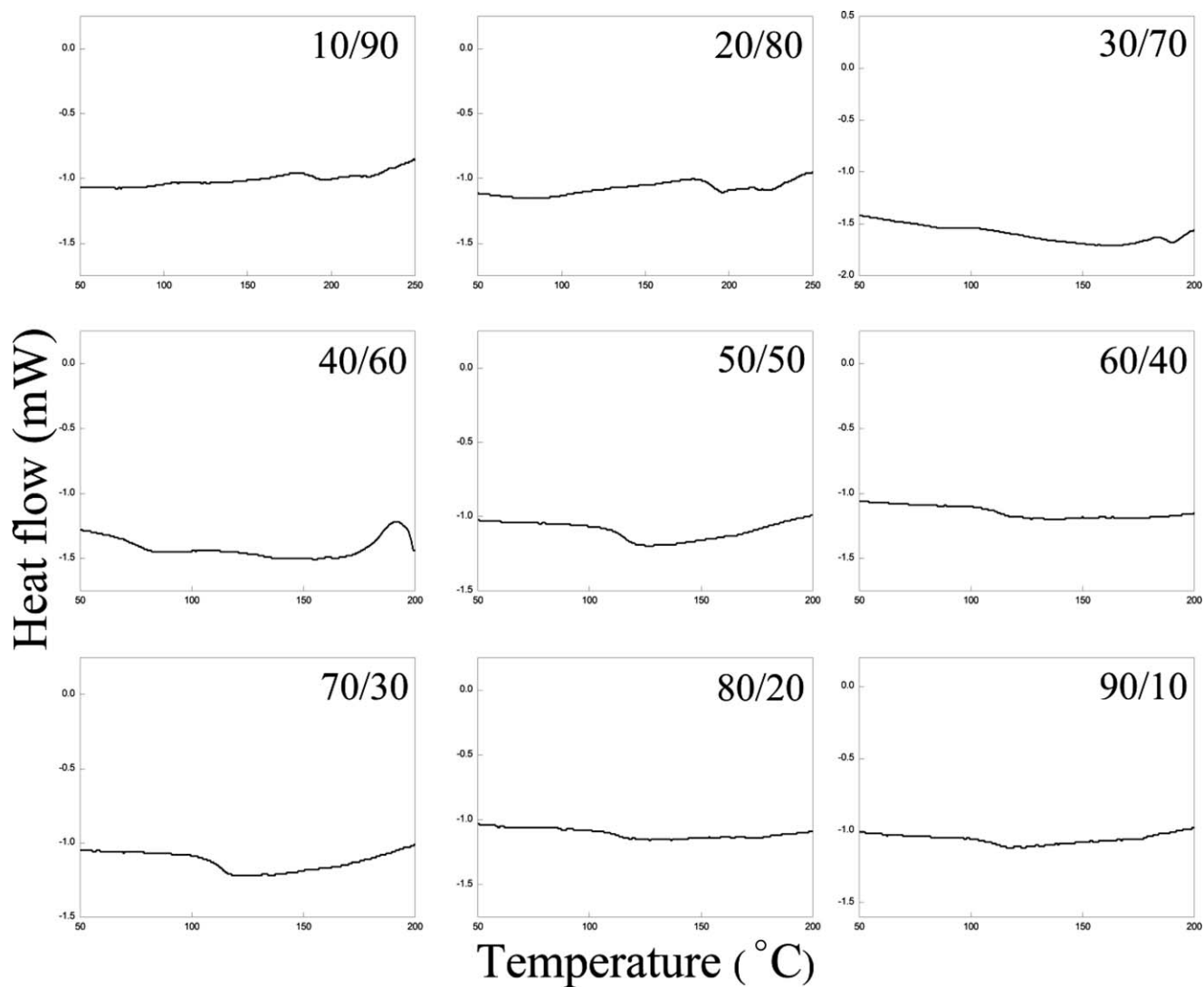


Figure 4. DSC scans of PMMA/CA blends.

Table II. Thermal Properties of PMMA/CA Blends

Sample	PMMA (wt %)	$T_g$ (°C)	Fox equation	Gordon-Taylor equation
0/100	0	191.78	191.78	191.78
10/90	10	190.27	177.83	165.09
20/80	20	182.97	165.77	148.76
30/70	30	128.19	155.24	137.73
40/60	40	125.92	145.97	129.78
50/50	50	115.15	137.74	123.78
60/40	60	113.61	130.39	119.09
70/30	70	111.8	123.79	115.32
80/20	80	111.34	117.82	112.23
90/10	90	111.24	112.40	109.65
100/0	100	107.46	107.46	107.46

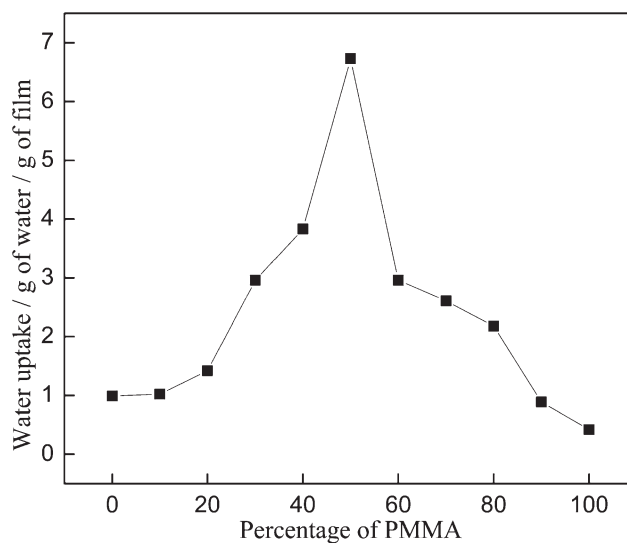


Figure 5. Water absorption of PMMA/CA blends.

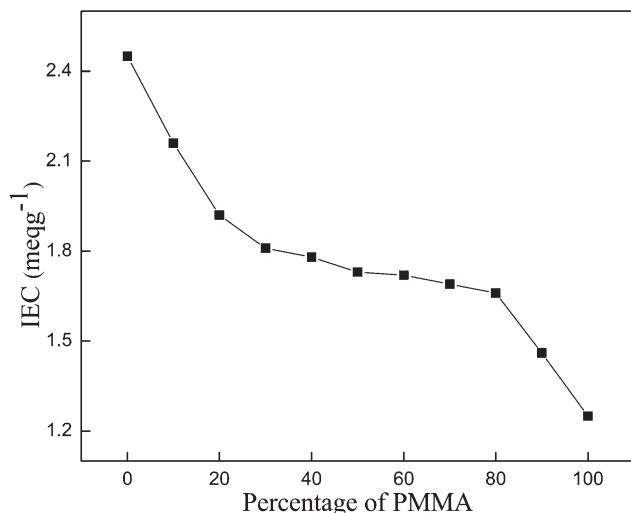


Figure 6. The variation of IEC values in the PMMA/CA blends.

at this composition may be facilitating this specific feature. At other compositions the component polymers may be blending in a gradually more compact structured pattern with reduction in void volumes and hence in turn reducing the water absorption.

#### Ion Exchange Capacity Measurements

Ion exchange capacity (IEC) provides an indirect approximation for the ion exchangeable groups present in the pure and blend polymers which are responsible for proton conduction. The IEC values for the PMMA/CA blends are shown graphically in Figure 6.

From the figure it can be seen that the IEC values of the blends decrease with an increase in PMMA content. It is known that CA has exchangeable —OH groups. Hence it is evident that when PMMA content of the blend is increased, the number of replaceable sites available in the blend would decrease and hence the decrease in the IEC of the blends.

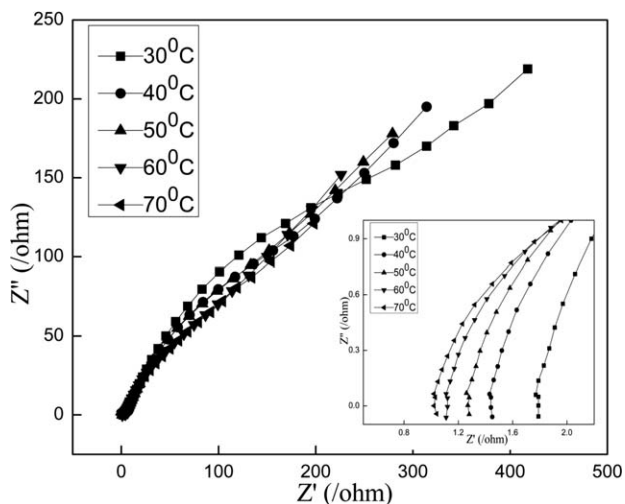
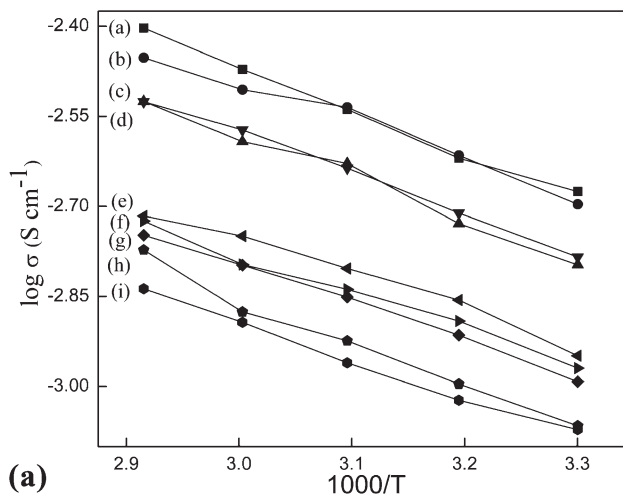
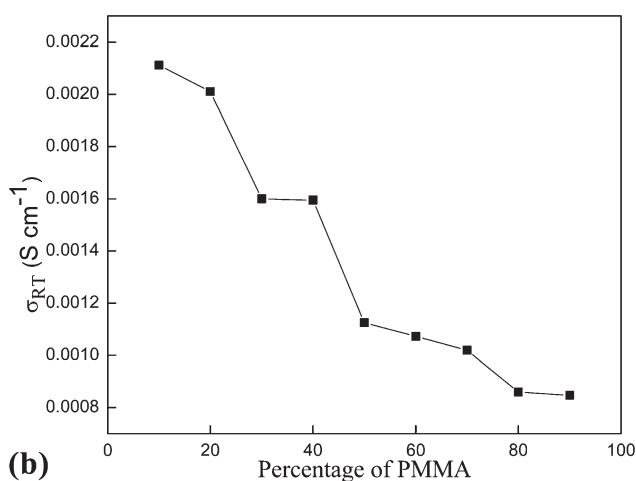


Figure 7. AC impedance spectra of 50/50 PMMA/CA blend at different temperatures.



(a)



(b)

Figure 8. (a) Arrhenius plots for conductivity  $\sigma$  of (a) 10/90, (b) 20/80, (c) 30/70, (d) 40/60, (e) 50/50, (f) 60/40, (g) 70/30, (h) 80/20, (i) 90/10 PMMA/CA blends. (b) Room temperature conductivity values of PMMA/CA blends.

#### Electrochemical Impedance Spectroscopic Studies

Electrochemical impedance spectroscopy is recently being widely applied in determining various material properties, prime among which are permittivity and conductivity. Figure 7 shows AC impedance spectra (Cole-Cole or Nyquist plots) of 50/50 PMMA/CA blend at different temperatures.

The impedance responses are typical of the electrolytes where the bulk resistance is the major contribution to the total resistance and only a minor contribution from grain boundary resistance. The straight lines inclined towards the real-axis representing the electrolyte–electrode double layer capacitance behavior are obtained for all the samples over the whole range of frequency evaluated.

**Proton Conductivity Measurement.** The variation of conductivity of the blends with temperature and room temperature conductivity of the blends are shown in Figure 8(a,b), respectively.

It has been observed that at 30°C, among the polyblends the blend with PMMA/CA 10/90 composition showed the highest

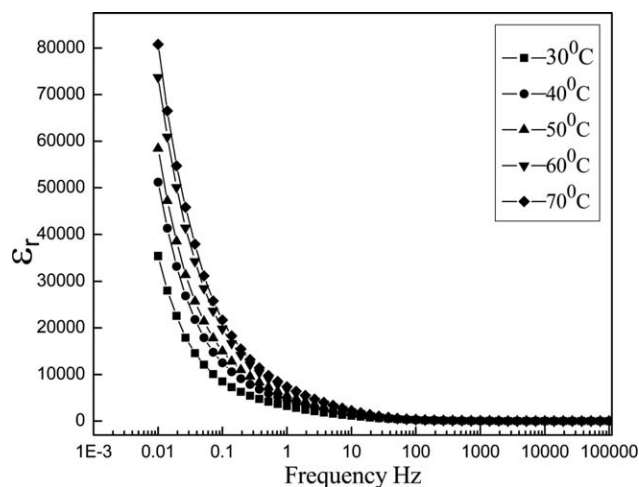


**Figure 9.** Variations of dielectric constant with frequency at different temperatures for 50/50 PMMA/CA blend.

proton conductivity value of  $2.11 \times 10^{-3} \text{ S cm}^{-1}$ . The proton conductivity increased as the temperature is increased in the measured temperature range between 30 and 70°C. Also, it has been found from impedance plots that as the temperature is increased, the bulk resistance  $R$  decreased resulting in an increase in the value of proton conductivity (Figure 7 inset). This may be mainly due to the fact that at higher temperature, there is an enhancement in the ion movement, favoring conductivity.

**Temperature Dependence of Ionic Conductivity.** It has been found that the proton conductivity of the blend films increased with increasing temperature for all the compositions. This may be mainly due to the fact that an increase in temperature increases the mobility of ions and this in turn increases the conductivity. Further, the vibrational motion of the polymer backbone and side chains, which becomes more vigorous with increase in temperature can also facilitate the conduction of ions. The increased amplitude of vibration brings the coordination sites closer to one another enabling the ions to hop from the occupied site to the unoccupied site with lesser energy required. Increase in amplitude of vibration of the polymer backbone and side chains can also increase the fraction of free volume in the polymer electrolyte system.<sup>18</sup> Druger et al.<sup>19,20</sup> have attributed the change in conductivity with temperature in solid polymer electrolyte to hopping model, which results in an increase in the free volume of the system. The hopping model either permits the ions to hop from one site to another or provides a pathway for ions to move. In other words, this facilitates translational motion of the ions. From this, it is clear that the ionic motion is due to translational motion/hopping facilitated by the polymer. The nonexistence of any unusual variation of conductivity indicates the existence of overall amorphous region.<sup>18</sup> This implies that coupling of the ion movement with the amorphous nature of the polymer is facilitating the conductivity in the blends.

Electrical conduction is a thermally activated process and follows the Arrhenius law

$$\sigma = \sigma_0 \exp \left[ -\frac{E_a}{kT} \right] \quad (9)$$

where,  $\sigma$  is the conductivity at a particular temperature,  $\sigma_0$  is the pre-exponential factor,  $k$  is the Boltzmann's constant, and  $T$  is the absolute temperature. As there is no sudden change in the value of conductivity with temperature it may be inferred that these blends do not undergo any phase transitions within the temperature range studied. The variation of conductivity of the studied blends with composition at room temperature shows that conductivity increased with increase in CA content in the blends. The overall trend is similar to that of IEC variation of the blends. A steep change in conductivity of the blends in the middle range of composition is also observed which is unlike that of IEC variation. It may also be recalled here that the water uptake behaviour also showed a different pattern in this region of composition. Hence the observed conductivity pattern of the blends may be attributed to the combined effects formation of specific structural features due to hydrogen bonding and variation of exchangeable group content in the blends which are facilitating the ion hopping through the polymer structure.

#### Dielectric Studies

The conductivity behavior of polymer electrolyte can be understood from dielectric studies.<sup>19</sup> The dielectric constant is a measure of stored charge. The variations of dielectric constant and dielectric loss with frequency at different temperatures have been shown in Figures 9 and 10, respectively.

There are no appreciable relaxation peaks observed in the frequency range employed in this study. Both dielectric constant and dielectric loss rise sharply at low frequencies indicating that electrode polarization and space charge effects have occurred confirming non-debye dependence.<sup>23,24</sup> On the other hand, at high frequencies, periodic reversal of the electric field occurs so fast that there is no excess ion diffusion in the direction of the field. Polarization due to charge accumulation decreases, leading to the observed decrease in dielectric constant and dielectric loss.<sup>25</sup> The dielectric constant and dielectric loss increase at higher temperatures due to the higher charge carrier density. As temperature increases, the degree of salt dissociation and

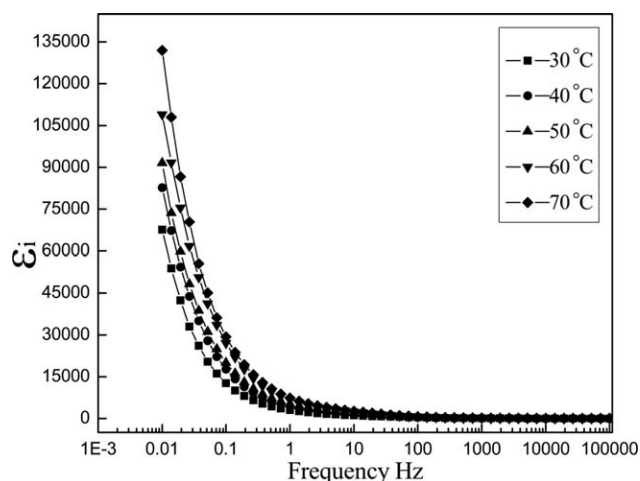


**Figure 10.** Variations of dielectric loss with frequency at different temperatures for 50/50 PMMA/CA blend.

redissociation of ion aggregates increases resulting in the increase in number of free ions or charge carrier density.

## CONCLUSIONS

In summary, the PMMA/CA blends have been prepared by solution casting method. Homogeneous polymer blend films are formed in the entire range of blend compositions and a single glass transition temperature is observed for each of the blends. The FTIR-ATR and DSC results suggest that these blend systems are miscible. The miscibility of the system may be due to the formation of a hydrogen bond between the carbonyl group of PMMA and the free hydroxyl group of CA.

The water uptake of blends increased with increasing PMMA content, whereas ion exchange capacity decreased with an increase in PMMA content. The trend in water uptake of the blends suggest the existence of inter molecular hydrogen bonding interactions between hydroxyl and carbonyl groups of CA and PMMA respectively. These specific interactions are considered to be responsible for continuous variation in water uptake in these blends. The variation in ion exchange capacity of the blends indicated that this property is mainly governed by the exchangeable group content present in the blends.

The maximum proton conductivity obtained at room temperature was  $2.11 \times 10^{-3} \text{ S cm}^{-1}$  for PMMA/CA 10/90 blend. The proton conductivity in these films has been attributed to the operation of hopping model type of mechanism. The dielectric studies of the blends suggest the absence of relaxation phenomenon. These materials may also be used as bioblends.

## ACKNOWLEDGMENTS

H.S. Sreekantha Jois is grateful to NITK Surathkal for the award of a research fellowship.

## REFERENCES

1. Kuo, S. W.; Chang, F. C. *Macromolecules* **2001**, *34*, 5224.
2. Kuo, S. W.; Tung, P.-H.; Chang, F.-C. *Macromolecules* **2006**, *39*, 9388.
3. Silva, P.; Albano, C.; Perera, R.; González, J.; Ichazo, M. *Nucl. Instrum. Meth. B* **2004**, *226*, 320.
4. Macaúbas, P. H. P.; Demarquette, N. R. *Polymer* **2001**, *42*, 2543.
5. Mohamed, A.; Gordon, S. H.; Biresaw, G. *Polym. Degrad. Stabil.* **2007**, *92*, 1177.
6. Selvakumar, M.; Bhat, D. K.; Renganathan, N. G. *J. Appl. Polym. Sci.* **2009**, *111*, 452.
7. Selvakumar, M.; Bhat, D. K. *Asian J. Chem.* **2011**, *23*, 1474.
8. Bhatt, A. S.; Bhat, D. K. *Polym. Bull.* **2012**, *68*, 253.
9. Bhatt, A. S.; Bhat, D. K.; Santosh, M. S.; Tai, C.-W. *J. Mater. Chem.* **2011**, *21*(35), 13490.
10. Sahu, A. K.; Selvarani, G.; Bhat, S. D.; Pitchumani, S.; Sridhar, P.; Shukla, A. K.; Narayanan, N.; Banerjee, A.; Chandrakumar, N. *J. Membr. Sci.* **2008**, *319*, 298.
11. White, A. J.; Filiako, F. E. *J. Polym. Sci. Pol. Lett.* **1982**, *20*, 525.
12. Shapiro, Y. E. *Bull. Magn. Reson.* **1972**, *7*, 27.
13. Gong, S.; Ma, H.; Wan, X. *Polym. Int.* **2006**, *55*, 1420.
14. He, Y.; Zhu, B.; Inoue, Y. *Prog. Polym. Sci.* **2004**, *29*, 1021.
15. Gordon, M.; Taylor, J. *J. Appl. Chem.* **1952**, *2*, 493.
16. Shirahase, T.; Komatsu, Y.; Tominaga, Y.; Asai, S.; Sumita, M. *Polymer* **2006**, *47*, 4839.
17. Fox, T.G. *Bull. Am. Phys. Soc.* **1956**, *1*, 123.
18. Aziz, S. B.; Abidin, Z. H. Z.; Arof, A. K. *Physica B* **2010**, *405*, 4429.
19. Druger, S. D.; Nitzam, A.; Ratner, M. A. *J. Chem. Phys.* **1983**, *79*, 3133.
20. Druger, S. D.; Ratner, M. A.; Nitzam, A. *Phys. Rev. B* **1985**, *31*, 3939.
21. Cowie, J. M. G.; Spence, G. H. *Solid State Ionics* **1998**, *109*, 139.
22. Ramesh, S.; Yahya, A. H.; Arof, A. K. *Solid State Ionics* **2002**, *152-153*, 291.
23. Qian, X.; Gu, N.; Cheng, Z.; Yang, X.; Wang, E.; Dong, S. *Electrochim. Acta* **2001**, *46*, 1829.
24. Govindaraj, G.; Baskaran, N.; Shahi, K.; Monoravi, P. *Solid State Ionics* **1995**, *76*, 47.
25. Ramesh, S.; Arof, A. K. *J. Power Sources* **2001**, *99*, 41.